

**This is an electronic reprint of the original article.
This reprint *may differ* from the original in pagination and typographic detail.**

Author(s): Delion, Doru-Sabin; Suhonen, Jouni

Title: Unified description of $2+_{-1}$ states within the deformed quasiparticle random-phase approximation

Year: 2013

Version:

Please cite the original version:

Delion, D.-S., & Suhonen, J. (2013). Unified description of $2+_{-1}$ states within the deformed quasiparticle random-phase approximation. *Physical Review C*, 87(2), Article 024309. <https://doi.org/10.1103/PhysRevC.87.024309>

All material supplied via JYX is protected by copyright and other intellectual property rights, and duplication or sale of all or part of any of the repository collections is not permitted, except that material may be duplicated by you for your research use or educational purposes in electronic or print form. You must obtain permission for any other use. Electronic or print copies may not be offered, whether for sale or otherwise to anyone who is not an authorised user.

Unified description of 2_1^+ states within the deformed quasiparticle random-phase approximation

D. S. Delion^{1,2,3} and J. Suhonen⁴

¹“Horia Hulubei” National Institute of Physics and Nuclear Engineering, 407 Atomiștilor, Bucharest-Măgurele, RO-077125, România

²Academy of Romanian Scientists, 54 Splaiul Independenței, Bucharest, RO-050094, România

³Bioterra University, 81 Gârlei str., Bucharest, RO-013724, România

⁴Department of Physics, University of Jyväskylä, POB 35, FIN-40351, Jyväskylä, Finland

(Received 2 December 2012; revised manuscript received 14 January 2013; published 13 February 2013)

We describe low-lying collective states in deformed even-even nuclei within a deformed quasiparticle random-phase approximation (dQRPA) by using a single-particle basis with good angular momentum. The statistical factors, accounting for the level occupancy, appear in the dQRPA in a natural way as rotation coefficients that take the intrinsic system to the laboratory system. We have used our model by performing a systematic analysis of E2 transitions from the first 2^+ state to the ground state for all superfluid nuclei in the range $50 < Z \leq 100$ by using a common charge polarization parameter $\chi = 0.2$. In spite of its similarity to the QRPA, this method is able to describe in an unified way gross features of electromagnetic transitions from vibrational to rotational nuclei.

DOI: [10.1103/PhysRevC.87.024309](https://doi.org/10.1103/PhysRevC.87.024309)

PACS number(s): 21.10.Re, 21.60.Jz, 23.20.Lv

I. INTRODUCTION

The many-body problem of deformed systems is a challenge for nuclear theory. In nuclear structure, the microscopic approaches dealing with deformed nuclei are based on the Nilsson model [1], describing single-particle (sp) dynamics in an intrinsic system of cylindrical symmetry. It provides a basis for the microscopic description of collective states in deformed systems. One of the most popular approaches to describe collective excitations is the quasiparticle random-phase approximation (QRPA) [2]. In deformed nuclei the calculations are performed in the intrinsic system of coordinates and therefore the physical states with good angular momentum are given by the projection procedure [3]. This method, called projection after variation, was widely used to describe a large variety of collective excitations, like the Gamow-Teller 1^+ resonance in the context of double-beta-decay processes [4–7], low-lying states in neutron-rich nuclei [8–10], the linear response function [11], giant resonances [12–14], the pygmy resonance [15], and magnetic properties of nuclei [16]. Let us also mention in this context the pseudo-SU(3) model, used to describe the double-beta-decay process in deformed nuclei [17].

A more exact but much more complex method is to use projected wave functions before the variational procedure, as done for instance in the method of variation after mean-field projection in realistic model spaces (VAMPIR) [18]. This approach is able to describe very complex effects, like the shape coexistence phenomenon [19].

Special attention was paid to the analysis of the first-excited 2^+ state in even-even nuclei by using the projected generator coordinate method [20,21].

Reference [22] proposed an alternative, relatively simple approach where the product between the spherical sp orbital and core wave function (described by a deformed coherent state), projected to a given angular momentum, is considered as a basis state for the many-body problem. In this way, many-particle–many-hole configurations are taken into account in an effective way due to the fact that the sp states are “dressed” by core wave functions. The resulting equations of motion have

formally a similar form as the ones corresponding to a spherical system. Later on, this method was used to describe various collective excitations in deformed nuclei, like two-neutrino double beta decay [23–25], magnetic collective states [26], and collective excitations in atomic clusters [27].

The purpose of the present paper is to generalize the approach of Ref. [22] by using a particle-core wave function coupled to a given angular momentum. In the Sec. II we give the necessary theoretical background and in Sec. III we apply it to describe electromagnetic transitions from collective 2_1^+ states for even-even vibrational, transitional, and rotational nuclei.

II. THEORETICAL BACKGROUND

In order to describe a deformed many-body system we will use an sp basis with good angular momentum:

$$a_{\tau njm}^\dagger(\Omega) = \sum_{Jk} X_{\tau nj}^{Jk} [D_{J0}^{J*}(\Omega) \otimes c_{\tau k}^\dagger]_{jm}, \quad (2.1)$$

in terms of spherical orbitals $c_{\tau km}^\dagger$, where τ is the isospin index, $k \rightarrow (\epsilon, l, k)$ has the meaning of sp energy ϵ , angular momentum l , and total spin k . Notice that the angular momentum coupling of the Wigner function is performed over the first projection, denoted by a dot in the above relation. Here, n denotes the eigenvalue index and the angular momentum coupling is considered over the laboratory projection M of the normalized Wigner function $D_{MK}^J(\Omega)$, while the intrinsic projection is $K = 0$.

The operators satisfy the following fermionic condition, written in the following form:

$$\begin{aligned} \langle \{a_{\tau njm}, a_{\tau n' j' m'}^\dagger\} \rangle_C &\equiv \int \{a_{\tau njm}(\Omega), a_{\tau n' j' m'}^\dagger(\Omega)\} d\Omega \\ &= \delta_{nn'} \delta_{jj'} \delta_{mm'}, \end{aligned} \quad (2.2)$$

pointing out on the necessity to use the integration over Euler angles in deriving many-body equations. The expansion

coefficients $X_{\tau nj}^{Jk}$ are found by diagonalizing the multipole-multipole core-particle interaction $r^\lambda [Y_\lambda(\Omega) \otimes Y_\lambda(\hat{r})]_0$.

In a simpler approach one supposes the adiabaticity, where the intrinsic spin sp projection ν is conserved. In this case the amplitudes are given by (see Chapter 4.7 in Ref. [28])

$$X_{\tau nj}^{Jk} = (-)^{j+\nu} \sqrt{2} \langle j\nu; k-\nu | J0 \rangle x_{\tau k\nu}^{(n)}, \quad (2.3)$$

in terms of Clebsch-Gordan coefficients and standard Nilsson amplitudes.

Next we will investigate 2_1^+ collective states within a deformed QRPA, by using the pairing plus quadrupole-quadrupole residual two-particle interaction and the deformed basis (2.1). We call this approach the dQRPA method. The dQRPA generalizes similar investigations performed by using the standard spherical QRPA code [29,30]. In this way it is possible to avoid the complicated problem of projecting out two-quasiparticle excitations of a deformed ground state. In our calculations we will consider the ‘‘yrast’’ Nilsson states with $j = \nu$ in Eq. (2.3) by dropping the index ν in our further notations.

Let us consider now the residual two-body interaction. The most general form, written in terms of the deformed basis (2.1), is given by

$$H_{\text{int}} = \sum_{\tau\tau'} \sum_{\lambda_0\lambda\lambda'} G_{\tau\tau'}^{\lambda_0\lambda\lambda'} (n_1 j_1 n'_1 j'_1; n_2 j_2 n'_2 j'_2) \times \{ \mathcal{D}_{.K}^{\lambda_0} \otimes [(a_{\tau n_1 j_1}^\dagger \otimes a_{\tau' n'_1 j'_1}^\dagger)_\lambda \otimes (a_{\tau n_2 j_2}^\dagger \otimes a_{\tau' n'_2 j'_2}^\dagger)_{\lambda'}]_{\lambda_0} \}_{0}. \quad (2.4)$$

The matrix elements are given by the integration of the product between the used two-body potential, single-particle wave functions, written in the representation (2.1), and the Wigner function. In our approach we will use a simplified separable form of the interaction, rewritten in the particle-hole representation as follows:

$$H_{\text{int}} \rightarrow H_Q = \sum_{\tau\tau'} \sum_{\lambda_0\lambda\lambda'} F_{\tau\tau'}^{\lambda_0\lambda\lambda'} [\mathcal{D}_{.K}^{\lambda_0} \otimes (Q_{\tau\lambda} \otimes Q_{\tau'\lambda'})_{\lambda_0}]. \quad (2.5)$$

The basic ingredients of our approach are the multipole operators, written in the deformed (nj) representation as

$$Q_{\tau\lambda\mu} = \sum_{12} \frac{\langle \tau n_1 j_1 || Q_\lambda || \tau n_2 j_2 \rangle_C}{\sqrt{2\lambda+1}} (a_{\tau n_1 j_1}^\dagger \otimes \tilde{a}_{\tau n_2 j_2})_{\lambda\mu}, \quad (2.6)$$

where the index C denotes the integration over the core Euler angles Ω , similar to Eq. (2.2). By using Eq. (2.1), one obtains the reduced matrix element of this operator in terms of standard spherical reduced matrix elements as follows:

$$\langle \tau n_1 j_1 || Q_\lambda || \tau n_2 j_2 \rangle_C = \hat{j}_1 \hat{j}_2 \sum_{Jk_1 k_2} X_{\tau n_1 j_1}^{Jk_1} X_{\tau n_2 j_2}^{Jk_2} (-)^{k_1+j_2+\lambda-J} \times W(j_1 k_1 j_2 k_2; J \lambda) \langle \tau k_1 || Q_\lambda || \tau k_2 \rangle, \quad (2.7)$$

where $\hat{j} = \sqrt{2j+1}$ and W is the standard Racah symbol. In the case of monopole operators the above relation for the band head $J = 0$ and $k = j$ can be written in terms of the largest

Nilsson component and has a simple form

$$\langle \tau n_1 j_1 || Q_0 || \tau n_2 j_2 \rangle_C = \delta_{12} \frac{2(x_{\tau j_1}^{n_1})^2}{2j_1+1} \langle \tau j_1 || Q_0 || \tau j_1 \rangle. \quad (2.8)$$

Thus, the factor multiplying the spherical reduced matrix element in Eq. (2.7) automatically contains the ‘‘statistical factors,’’ which become $\frac{2}{2j+1}$ for the monopole case. This factor, well known in proton emission [see Eq. (4.66) in Ref. [28]], was introduced in Ref. [22] ad hoc by using purely statistical reasoning. Here, we suppose the validity of the adiabatic assumption, due to the fact that the core states have low angular momenta. This condition keeps valid the intrinsic pairing condition, but seen in the laboratory system of coordinates. We will restrict ourselves to a monopole pairing Hamiltonian with constant strengths for protons and neutrons, respectively, by recoupling pp components with higher multipolarity into the corresponding ph terms. Thus, the pairing Hamiltonian can be approximated by the following ansatz in the deformed (nj) representation

$$H_P \rightarrow \sum_{\tau} \sum_{nj} (e_{\tau nj} - \Lambda_{\tau}) \frac{2}{2j+1} N_{\tau nj} - \frac{1}{4} \sum_{\tau} \sum_{n j n' j'} G_{\tau n j n' j'} \frac{2}{2j+1} P_{\tau nj}^\dagger \frac{2}{2j'+1} P_{\tau n' j'}, \quad (2.9)$$

where

$$e_{\tau nj} = \epsilon_{\tau nj} (x_{\tau j}^{(n)})^2, \quad (2.10)$$

$$G_{\tau n j n' j'} = G_{\tau} [x_{\tau j}^{(n)} x_{\tau j'}^{(n')}]^2.$$

Here $N_{\tau nj}$ denotes the particle-number operator and the monopole pairing operator is given by $P_{\tau nj}^\dagger = \sqrt{2j+1} (a_{\tau nj}^\dagger \otimes a_{\tau nj}^\dagger)_0$. One can easily see that in the case of a common value of the Nilsson amplitude, one obtains the standard Hamiltonian with shifted sp energies and a renormalized constant pairing strength. Indeed, this is approximately true for a given deformation concerning the orbitals around the Fermi level, which play the leading role in determining the pairing gap. In our calculations we will use this approximation.

It is worth mentioning that Eq. (4.5) of Ref. [22] has a similar ansatz with our Eq. (2.9), but the paired states are spherical orbitals ‘‘dressed’’ by core states. In our case the paired states are deformed Nilsson orbitals in the laboratory system, dressed by the core states. Thus, it becomes possible to use the replacement $2j+1 \rightarrow 2$ in spherical BCS equations in order to obtain the same relations as for the deformed case. In the quasiparticle representation

$$a_{\tau njm}^\dagger = u_{\tau nj} \alpha_{\tau njm}^\dagger + v_{\tau nj} \alpha_{\tau nj-m} (-)^{j-m}, \quad (2.11)$$

the multipole operator becomes

$$Q_{\tau\lambda\mu} = \sum_{n_1 j_1 \leq n_2 j_2} \xi_{\tau 12}^\lambda [\bar{A}_{\lambda\mu}^\dagger(\tau_{12}) + (-)^{\lambda-\mu} \bar{A}_{\lambda-\mu}(\tau_{12})], \quad (2.12)$$

in terms of the normalized pair quasiparticle operator

$$\bar{A}_{jm}^\dagger(\tau_{12}) = \frac{1}{\sqrt{1 + \delta_{n_1 n_2} \delta_{j_1 j_2}}} (\alpha_{\tau n_1 j_1}^\dagger \otimes \alpha_{\tau n_2 j_2}^\dagger)_{jm}, \quad (2.13)$$

where we used the short-hand notation $\tau_{12} = (\tau n_1 j_1 n_2 j_2)$ and

$$\xi_{\tau_{12}}^\lambda = \frac{\langle \tau n_1 j_1 || Q_\lambda || \tau n_2 j_2 \rangle_C}{\sqrt{(2\lambda + 1)(1 + \delta_{n_1 n_2} \delta_{j_1 j_2})}} \times (u_{\tau n_1 j_1} v_{\tau n_2 j_2} + v_{\tau n_1 j_1} u_{\tau n_2 j_2}). \quad (2.14)$$

As a result of the deformation, the residual Hamiltonian (2.5) couples QRPA phonons of multipole λ

$$\Gamma_{\lambda\mu}^\dagger(\nu) = \sum_\tau \sum_{n_1 j_1 \leq n_2 j_2} [\mathcal{X}_\lambda^{(\nu)}(\tau_{12}) \bar{A}_{\lambda\mu}^\dagger(\tau_{12}) - \mathcal{Y}_\lambda^{(\nu)}(\tau_{12}) \bar{A}_{\lambda-\mu}(\tau_{12}) (-)^{\lambda-\mu}], \quad (2.15)$$

with phonons of other multipoles leading to the general phonon

$$D_{\lambda\mu}^\dagger(\nu) = \sum_{\lambda_0 \lambda'} Z_{\lambda_0 \lambda'}^{(\nu)} [\mathcal{D}_{\lambda_0}^{\lambda_0} \otimes \Gamma_{\lambda'}^\dagger(\nu)]_{\lambda\mu}. \quad (2.16)$$

In this work we will restrict ourselves to the lowest term with $\lambda_0 = 0$ and $\lambda = \lambda'$. Thus, we will use the pairing plus multipole-multipole Hamiltonian

$$\begin{aligned} H &= H_P - H_Q \\ &= H_P - \frac{1}{2} \sum_\lambda \sum_{\tau\tau'} F_{\tau\tau'}^\lambda \sqrt{2\lambda + 1} (Q_{\tau\lambda} \otimes Q_{\tau'\lambda})_0, \end{aligned} \quad (2.17)$$

and the QRPA equations become decoupled. We further assume that a similar averaged rule (2.2) can also be applied to the commutator of quasiparticle pair operators (2.14). By minimizing the functional

$$E_\lambda(\nu) = \frac{\langle [\Gamma_\lambda(\nu), H, \Gamma_\lambda^\dagger(\nu)] \rangle_C}{\langle [\Gamma_\lambda(\nu), \Gamma_\lambda^\dagger(\nu)] \rangle_C}, \quad (2.18)$$

where the expectation values include the integration over Ω , the QRPA amplitudes are given by (the dQRPA) equations of motion which are formally similar to those of the spherical version:

$$\begin{pmatrix} \mathcal{A}_\lambda & \mathcal{B}_\lambda \\ -\mathcal{B}_\lambda & -\mathcal{A}_\lambda \end{pmatrix} \begin{pmatrix} \mathcal{X}_\lambda^{(\nu)} \\ \mathcal{Y}_\lambda^{(\nu)} \end{pmatrix} = E_\lambda(\nu) \begin{pmatrix} \mathcal{X}_\lambda^{(\nu)} \\ \mathcal{Y}_\lambda^{(\nu)} \end{pmatrix}. \quad (2.19)$$

The dQRPA matrix elements are given by the following symmetrized double commutators:

$$\begin{aligned} \mathcal{A}_\lambda(\tau_{12}\tau'_{12}) &= \langle [\bar{A}_{\lambda\mu}(\tau_{12}), H, \bar{A}_{\lambda\mu}^\dagger(\tau'_{12})] \rangle_C \\ &= \delta_{\tau_{12}\tau'_{12}} (E_{\tau n_1 j_1} + E_{\tau n_2 j_2}) - F_{\tau\tau'}^\lambda \xi_{\tau_{12}}^\lambda \xi_{\tau'_{12}}^\lambda, \\ \mathcal{B}_\lambda(\tau_{12}\tau'_{12}) &= -\langle [\bar{A}_{\lambda\mu}(\tau_{12}), H, \bar{A}_{\lambda-\mu}(\tau'_{12}) (-)^{\lambda-\mu}] \rangle_C \\ &= -F_{\tau\tau'}^\lambda \xi_{\tau_{12}}^\lambda \xi_{\tau'_{12}}^\lambda, \end{aligned} \quad (2.20)$$

and they contain quasiparticle energies $E_{\tau n j} = [(e_{\tau n j} - \Lambda_\tau)^2 + \Delta_\tau^2]^{1/2}$, labeled by the eigenvalue index n , and the factors $\xi_{\tau_{12}}^\lambda$ (2.14) featuring the deformed matrix elements. As we will show latter, in spite of the similarity to the spherical QRPA, this formalism is more general. It is able to describe in a unified way low-lying excitations not only in spherical but also in deformed systems.

The strength of an electric transition, connecting the dQRPA eigenstate ν to the ground state, is characterized by

the $B(E\lambda)$ value defined by

$$B(E\lambda : \nu \rightarrow 0) = \frac{1}{2\lambda + 1} |\langle 0 || \hat{T}_\lambda || \nu \rangle_C|^2, \quad (2.21)$$

with the reduced matrix element

$$\begin{aligned} \langle 0 || \hat{T}_\lambda || \nu \rangle_C &= \sqrt{2\lambda + 1} \sum_\tau e_\tau \\ &\times \sum_{n_1 j_1 \leq n_2 j_2} \xi_{\tau_{12}}^\lambda [\mathcal{X}_\lambda^{(\nu)}(\tau_{12}) + \mathcal{Y}_\lambda^{(\nu)}(\tau_{12})], \end{aligned} \quad (2.22)$$

where e_τ are the effective charges

$$e_\pi = e(1 + \chi), \quad e_\nu = \chi, \quad (2.23)$$

expressed in terms of the polarization parameter χ .

III. NUMERICAL APPLICATION

We have applied the dQRPA approach to describe the $B(E2)$ values of decays from the 2_1^+ collective state to the ground state in superfluid vibrational, transitional, and rotational nuclei. Nilsson states in the intrinsic system of coordinates were provided by diagonalizing the axially symmetric quadrupole interaction $\beta m_N \omega^2 r^2 Y_{20}(\theta')$. As a basis we used the eigenstates of the spherical Woods-Saxon potential with a universal set of parameters [31] plus a Coulomb interaction for protons. The deformation parameters were taken from Ref. [32] and the experimental pairing gaps were estimated by using binding-energy data [32] of neighboring nuclei. The pairing gaps G_τ in Eq. (2.10) were automatically determined. The quadrupole-quadrupole coupling strengths $F_{\tau\tau'}^2$, defined by Eq. (2.17), were considered equal, as in the classical Ref. [29]. The common value was determined from the experimental 2_1^+ energy [33] for each nucleus by using the standard dispersion-relation technique for separable interactions. For the polarization parameter in Eq. (2.23) we adopted the (universal) value $\chi = 0.2$.

For the spherical sp basis we used five orbitals below and five above the Fermi level giving about 50 QRPA pairs, while for the deformed one we used an equivalent space provided by 15 levels below and 15 above the Fermi level, i.e., about 350 pairs in the dQRPA basis. As a test we analyzed the energy-weighted strength function, defined by the product

$$EWSF = E(\nu) B(E2 : \nu \rightarrow 0), \quad (3.1)$$

as a function of the QRPA eigenvalues $E(\nu)$. The result for the vibrational nucleus ^{130}Te , given by the standard spherical QRPA code, is plotted in Fig. 1(a). The similar result, but provided by the deformed QRPA code, with the deformation parameter $\beta = 0$, is given in Fig. 1(b). One sees that the two results practically coincide, proving the validity of the key ingredient of dQRPA, which is the reduced matrix element in the deformed basis, given by Eq. (2.7). As a reference, we give in Figs. 1(c) and 1(d) the same plots, but for the rotational nucleus ^{240}Pu . Here, the deformation parameter $\beta = 0.22$ was used in the dQRPA calculation. As is well visible the results of the spherical QRPA and dQRPA are completely different.

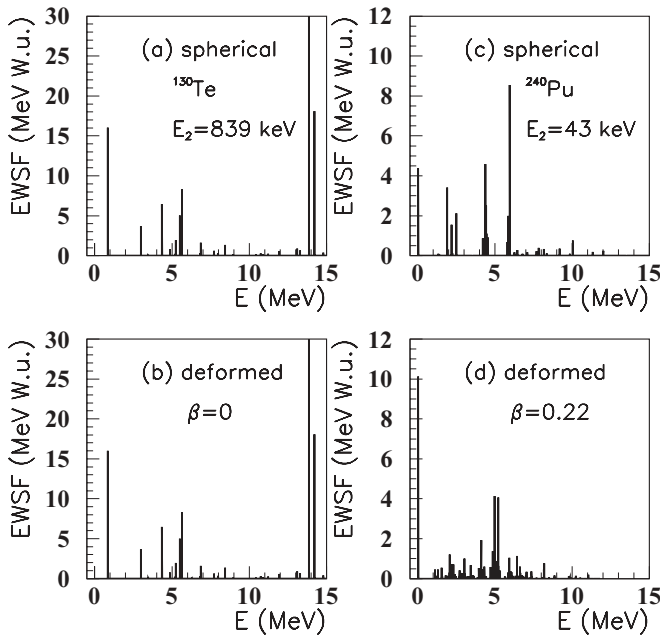


FIG. 1. Energy-weighted strength function (3.1) for (a) the spherical QRPA and (b) dQRPA in the case of the vibrational nucleus ^{130}Te . Similar plots are given in panels (c) and (d) for the rotational nucleus ^{240}Pu , by using the deformation parameter of the deformed field from Ref. [32].

Notice that the strength corresponding to the 2_1^+ state becomes significantly larger.

In order to analyze the differences between the spherical and deformed approaches, we have investigated the E2 decay properties of the 2_1^+ states in superfluid even-even nuclei for the region $50 < Z \leq 100$. We have divided the data into two sets separated by the magic number $Z = 82$.

In Fig. 2(a) we give by the open symbols the experimental $B(E2)$ values [33] in the region $50 \leq Z \leq 82$ (111 values), while by the filled symbols we indicate the $B(E2)$ values for $82 < Z \leq 100$ (27 values). The correspondence between the charge number of the isotopic chains we analyzed, the associate neutron numbers and the interval of the index values n is given in Table I.

In Fig. 2(b) are plotted the results given by the spherical QRPA code. They reproduce the order of magnitude of the $B(E2)$ s in the region $50 \leq Z \leq 82$ (open symbols), containing mostly vibrational and transitional nuclei. The relative mean square error in this region is about 30%. In the region $82 < Z \leq 100$ (filled symbols), where most nuclei have small 2_1^+ energies and rotational spectra, the computed $B(E2)$ values are by a factor 2 to 3 lower, the mean-square error being about 100%. So, as expected, the spherical QRPA fails in reproducing the $B(E2)$ values for rotational nuclei. On the contrary, in Fig. 2(b) this region is much better reproduced by the dQRPA (filled symbols). Indeed, here the mean-square error decreases down to 25%. In order to enable a clear comparison, in Fig. 2(d) we show again the experimental values. The better agreement of the dQRPA results with the data can be explained by the summation over core states J in the reduced matrix element

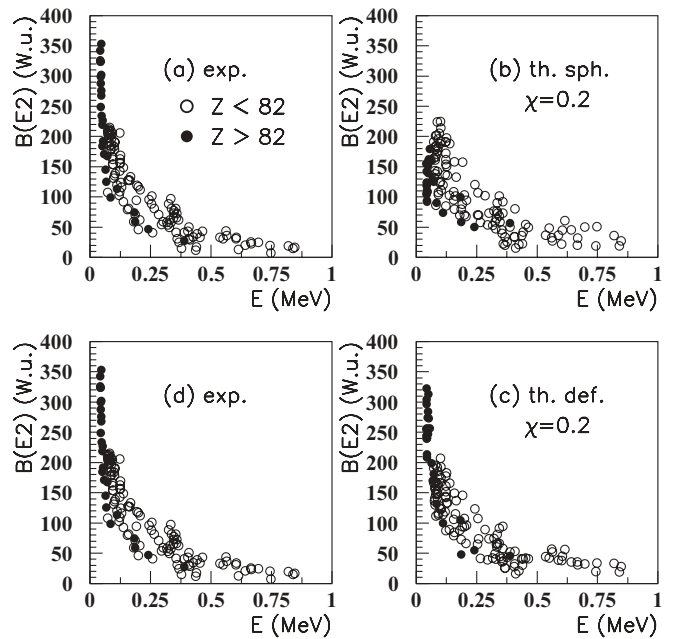


FIG. 2. Theoretical $B(E2)$ values given by the standard spherical QRPA (b) and the dQRPA (c) versus excitation energy. For a better comparison, in panels (a) and (d) are given the same experimental $B(E2)$ values [33].

given by Eq. (2.7). Indeed, by considering only the lowest yrast core state the $B(E2)$ results become lower, comparable to the spherical method. Thus, the core states play an important role in describing well deformed nuclei. In Fig. 3(a) we plotted the same data, but versus the quadrupole deformation parameter β . One notices different slopes for the two mentioned regions. This feature cannot be explained by the spherical QRPA given in Fig. 3(b), but it is nicely reproduced by dQRPA in Fig. 3(c).

Finally, in Fig. 4 we give the quadrupole-quadrupole coupling strength $F_{\tau\tau'}^2$ as a function of the mass number for the spherical case by filled symbols and deformed case by open symbols. The values are close to each other, especially in the region above $Z > 82$. Their bulk features can be approximated by the corresponding power laws, given in Fig. 4. As an interesting observation, notice that the strength of the deformed

TABLE I. Charge numbers and the corresponding intervals for neutron and index values.

Z	N	n	Z	N	n	Z	N	n
52	68–78	1–6	66	86–98	51–57	86	134–136	1–2
54	64–86	7–17	68	88–102	58–65	88	130–140	3–7
56	70–90	18–26	70	88–106	66–75	90	132–144	8–13
58	70–92	27–34	72	94–108	76–83	92	136–146	14–18
60	84–92	35–39	74	94–112	84–90	94	144–150	19–22
62	76–92	40–45	76	106–116	91–96	96	148–152	23–25
64	88–96	46–50	78	106–120	97–104	98	152–154	26–27
			80	104–124	105–111			

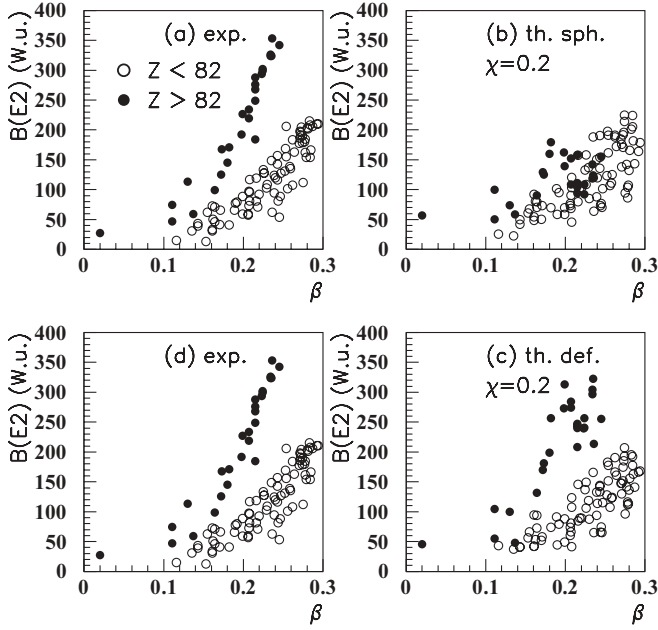


FIG. 3. Same as in Fig. 2, but versus the quadrupole deformation parameter of the deformed mean field [32].

interaction follows better a quadratic law in the region below the double-magic nucleus ^{208}Pb .

It is not the purpose of this paper to analyze the higher 2_k^+ states, predicted by QRPA eigenvalues. Anyway, let us mention that this approach is able to describe their gross features. In order to illustrate this fact, we plotted by open symbols in Fig. 5(a) spherical 2_k^+ QRPA eigenvalues, corresponding

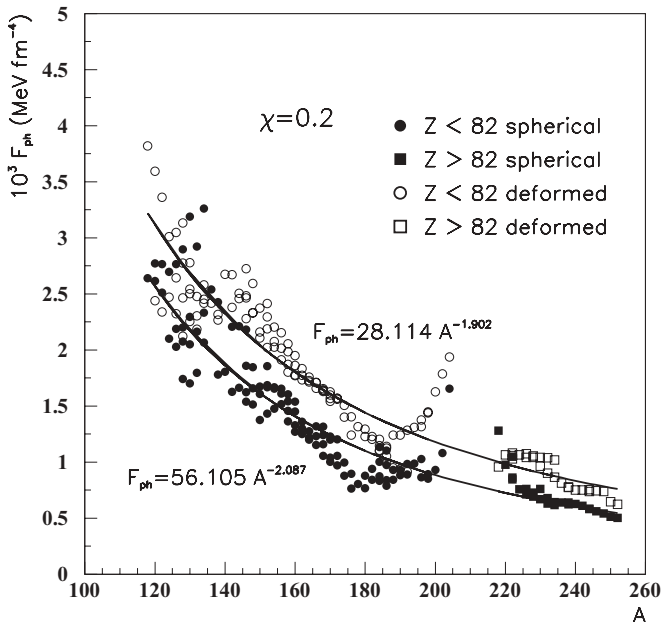


FIG. 4. Values of coupling strength multiplying the spherical QQ interaction (filled symbols) and the deformed QQ interaction (open symbols) versus the mass number. The corresponding fitting curves are also given.

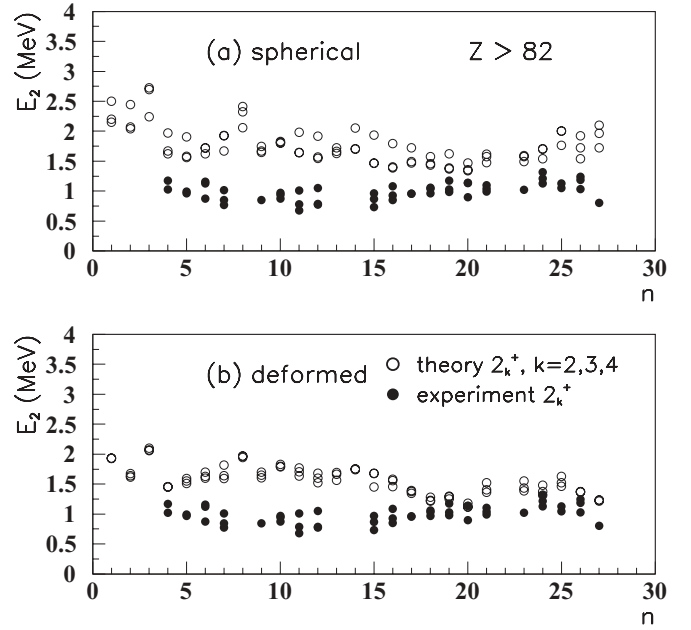


FIG. 5. (a) Energies of 2_k^+ states, $k = 2, 3, 4$ for spherical QRPA (open symbols) and the corresponding experimental values (filled symbols) as a function of states. The labels correspond to the isotopic chains given by the last three columns of the Table I. (b) Same as in (a) but for dQRPA.

to $k = 2, 3, 4$, for the region $Z > 82$. This region contains mainly well-deformed nuclei. As a comparison, there are given the corresponding available experimental values by filled symbols. One sees that the theoretical values display the same clustering features as the experimental ones ($k = 2, 3, 4$ eigenvalues are close to each other for each isotope), but they are higher, especially for $Z = 88$ and 90 isotopes. On the other hand, the corresponding dQRPA eigenvalues in Fig. 5(b) improve the situation. The electric transitions connecting these states to the ground state are much smaller in comparison to 2_1^+ states, i.e., between 0.1 and 0.4 W.u. (Weisskopf units) (depending on the excitation energy), thus reproducing the experimental order of magnitude. One has to keep in mind that we used a very simple approach by considering that all QQ strengths in Eq. (2.17) are equal. By using different coupling strengths it is of course possible to improve the agreement of higher 2_k^+ states with experiment.

IV. CONCLUSIONS

In conclusion, we described the quadrupole collective excitations in even-even nuclei within a common formalism, called the deformed QRPA (dQRPA), by using an sp basis with good angular momentum provided by the Nilsson states rotated into the laboratory frame of coordinates. Thus, the physical collective states are directly determined, without any additional projection procedure. The statistical factors, taking into account the level occupancy in the laboratory system, appear in a natural way within the dQRPA as rotation coefficients of the wave function when taking it from the

intrinsic to the laboratory system. We analyzed E2 transitions from the collective 2_1^+ state to the ground state for superfluid nuclei in the charge-number range $50 < Z \leq 100$ by using a single value $\chi = 0.2$ for the polarization charge. It turned out that, as expected, the standard spherical QRPA approach fails in describing rotational nuclei with $E_2 < 100$ keV. On the other hand, the dQRPA improves dramatically the description of the E2 transitions for these nuclei. Therefore the assumed adiabaticity seems to be a reasonable assumption in describing low-lying collective states. This relatively simple approach seems to be very promising in analyzing any kind of spin-multipole interaction, including magnetic type of

excitations and intraband transitions in deformed nuclei within the multipole-coupled approach given by Eq. (2.16). Further applications of the dQRPA are under way.

ACKNOWLEDGMENTS

This work was supported by the Academy of Finland under the Finnish Center of Excellence Program 2012-2017 (Nuclear and Accelerator Based Program at JYFL) and the grant PN-II-ID-PCE-2011-3-0092 of the Romanian Ministry of Education and Research. Discussions with Dorel Bucurescu (Bucharest) are gratefully acknowledged.

-
- [1] S. G. Nilsson, Kgl. Danske Videnskab. Selskab. Mat.-fys Medd. **29**, 16 (1955).
- [2] D. J. Rowe, *Phys. Rev.* **175**, 1283 (1968).
- [3] V. G. Soloviev, *Theory of Atomic Nuclei: Quasiparticles and Phonons* (Institute of Physics, Bristol, 1992).
- [4] F. Simkovic, L. Pacearescu, and A. Faessler, *Nucl. Phys. A* **733**, 321 (2004).
- [5] P. Sarriguren, O. Moreno, R. Alvarez-Rodriguez, and E. M. de Guerra, *Phys. Rev. C* **72**, 054317 (2005).
- [6] D. Fang, A. Faessler, V. Rodin, M. S. Yousef, and F. Simkovic, *Phys. Rev. C* **81**, 037303 (2010).
- [7] E. Ha and M.-K. Cheoun, *J. Korean Phys. Soc.* **59**, 1533 (2011).
- [8] K. Hagino, N. V. Giai, and H. Sagawa, *Nucl. Phys. A* **731**, 264 (2004).
- [9] K. Yoshida, M. Yamagami, and K. Matsuyanagi, *Nucl. Phys. A* **79**, 99 (2006).
- [10] K. Yoshida and N. V. Giai, *Phys. Rev. C* **78**, 064316 (2008).
- [11] C. Losa, A. Pastore, T. Dossing, E. Vigezzi, and R. A. Broglia, *Phys. Rev. C* **81**, 064307 (2010).
- [12] S. Peru and H. Goutte, *Phys. Rev. C* **77**, 044313 (2008).
- [13] J. Terasaki and J. Engel, *Phys. Rev. C* **82**, 034326 (2010).
- [14] M. Stoitsov, M. Kortelainen, T. Nakatsukasa, C. Losa, and W. Nazarewicz, *Phys. Rev. C* **84**, 041305(R) (2011).
- [15] S. Peru, H. Goutte, and J. F. Berger, *Nucl. Phys. A* **788**, 44 (2007).
- [16] H. Yakuta, E. Guliyev, M. Guner, E. Tabar, and Z. Zenginerler, *Nucl. Phys. A* **888**, 23 (2012).
- [17] J. Suhonen and O. Civitarese, *Phys. Rep.* **300**, 123 (1998).
- [18] E. Bender, K. W. Schmidt, and A. Faessler, *Nucl. Phys. A* **596**, 1 (1996).
- [19] A. Petrovici, *J. Phys. G* **37**, 064036 (2010).
- [20] B. Sabbey, M. Bender, G. F. Bertsch, and P.-H. Heenen, *Phys. Rev. C* **75**, 044305 (2007).
- [21] G. F. Bertsch, M. Girod, S. Hilaire, J.-P. Delaroche, H. Goutte, and S. Peru, *Phys. Rev. Lett.* **99**, 032502 (2007).
- [22] A. A. Raduta, D. S. Delion, and N. Lo Iudice, *Nucl. Phys. A* **551**, 93 (1993).
- [23] A. A. Raduta, A. Faessler, and D. S. Delion, *Nucl. Phys. A* **564**, 185 (1993).
- [24] A. A. Raduta, A. Escuderos, A. Faessler, E. Moya de Guerra, and P. Sarriguren, *Phys. Rev. C* **69**, 064321 (2004).
- [25] A. A. Raduta, C. M. Raduta, and A. Escuderos, *Phys. Rev. C* **71**, 024307 (2005).
- [26] A. A. Raduta, A. Escuderos, and E. Moya de Guerra, *Phys. Rev. C* **65**, 024312 (2002).
- [27] A. A. Raduta, R. Budaca, and Al. H. Raduta, *Phys. Rev. A* **79**, 023202 (2009).
- [28] D. S. Delion, *Theory of Particle and Cluster Emission* (Springer-Verlag, Berlin, 2010).
- [29] L. S. Kisslinger and R. A. Sorensen, *Rev. Mod. Phys.* **35**, 853 (1962).
- [30] J. Terasaki, J. Engel, and G. F. Bertsch, *Phys. Rev. C* **78**, 044311 (2008).
- [31] J. Dudek, W. Nazarewicz, and T. Werner, *Nucl. Phys. A* **341**, 253 (1980).
- [32] P. Moller and J. R. Nix, *Nucl. Phys. A* **272**, 502 (1995).
- [33] S. Raman, C. W. Nestor, Jr., and P. Tikkanen, *At. Data Nucl. Data Tables* **78**, 1 (2001).